Effect of embedment depth and stress anisotropy on expansion and contraction of cylindrical cavities

Hany El Naggar[1], Ph.D., P. Eng. and M. Hesham El Naggar[2], Ph.D., P. Eng.
[1]*Department of Civil Engineering – ALHOSN University, Abu Dhabi, UAE*
[2]*Department of Civil & Environmental Engineering – University of Western Ontario, Canada*

ABSTRACT
The semi-analytical solutions for expansion and contraction of cylindrical cavities in elasto-plastic dilatant soils developed by Yu and Houlsby (1991, 1995) were applied to a wide spectrum of applications from interpretations of pressuremeter tests in sand and the end bearing pressure of deep foundations to horizontal directional drilling (HDD). The main assumptions of these solutions are: 1) infinite medium; and 2) isotropic stress field everywhere (i.e., the coefficient of lateral earth pressure, Ko =1). For HDD applications, these assumptions are not justified for most installations, and the effect of any deviation from these assumptions needs to be evaluated. This paper investigates the effect of the free surface, the stress gradient, and the in-situ stress anisotropy (i.e. Ko≠1) on the displacements during expansion and contraction phases of cavities embedded in dilatant sands. A finite element model was built using the software Plaxis. The finite element was first verified for the case of infinite medium and isotropic stress field. The verified model was then used to examine the effects of the different influencing parameters of the HDD installation.

RÉSUMÉ
The semi-analytical solutions for expansion and contraction of cylindrical cavities in elasto-plastic dilatant soils developed by Yu and Houlsby (1991, 1995) were applied to a wide spectrum of applications from interpretations of pressuremeter tests in sand and the end bearing pressure of deep foundations to horizontal directional drilling (HDD). The main assumptions of these solutions are: 1) infinite medium; and 2) isotropic stress field everywhere (i.e., the coefficient of lateral earth pressure, Ko =1). For HDD applications, these assumptions are not justified for most installations, and the effect of any deviation from these assumptions needs to be evaluated. This paper investigates the effect of the free surface, the stress gradient, and the in-situ stress anisotropy (i.e. Ko≠ 1) on the displacements during expansion and contraction phases of cavities embedded in dilatant sands. A finite element model was built using the software Plaxis. The finite element was first verified for the case of infinite medium and isotropic stress field. The verified model was then used to examine the effects of the different influencing parameters of the HDD installation.

1 INTRODUCTION

Cavity expansion and contraction theories have significant practical implications in several engineering areas. For instance, the analysis of a cylindrical cavity has been applied to a wide spectrum of applications such as the interpretation of pressuremeter tests (e.g. Gibson & Anderson, 1961; Palmer, 1972; Hughes et al., 1977) and the end bearing pressure of deep foundations (e.g. Randolph et al., 1979), shaft capacity of tapered piles (El Naggar and Sakr, 2000) and to tunnelling (e.g. Yu and carter, 2002, Yu and Rowe, 1999). In addition, the semi-analytical solutions for expansion and contraction of cylindrical cavities in elasto-plastic dilatant soils developed by Yu and Houlsby (1991, 1995) were applied to horizontal directional drilling (HDD) (Fernando and Moore, 2002).

The main assumptions of these solutions are: 1) infinite medium; and 2) isotropic stress field everywhere (i.e. the coefficient of lateral earth pressure, K_o =1) (Yu and Houlsby 1991, 1995). For HDD applications, these assumptions are not justified for most installations, and the effect of any deviation from these assumptions needs to be evaluated.

This paper investigates the effect of three aspects, including: free surface conditions; stress gradient; and in-situ stress anisotropy (i.e. $K_o \neq 1$) on the displacements during expansion and contraction phases of cavities embedded in dilatant sands. A finite element model was built using the software Plaxis. The numerical model was first verified for the case of infinite medium and isotropic stress field. The verified model was then used to examine the effects of the different influencing parameters of the HDD installation.

2 CAVITY EXPANSION AND CONTRACTION THEORY

Yu and Houlsby (1991, 1995) used the Mohr-Coulomb yield criterion to derive an analytical solution for the expansion and contraction of a cylindrical cavity in a dilatant elasto-plastic soil. In this solution, the geometry of the problem is defined by the initial radius of the cavity, a_o, the radius at the end of the expansion phase, a_1, and the radius at the end of the contraction phase, a_2. The external radius of the plastic zone at the end of the expansion phase is d_1, while the external radius of the plastic zone at the end of the contraction phase is d_2.

Figure 1 shows the geometry of the expansion and contraction phases.

The properties of soil used to characterize its behaviour during different phases are: the elastic modulus, E; Poisson's ratio, v; adhesion, c; angle of internal friction, ϕ; dilation angle, ψ; and the initial pressure P_o, which is a function of the overburden pressure above the point of interest.

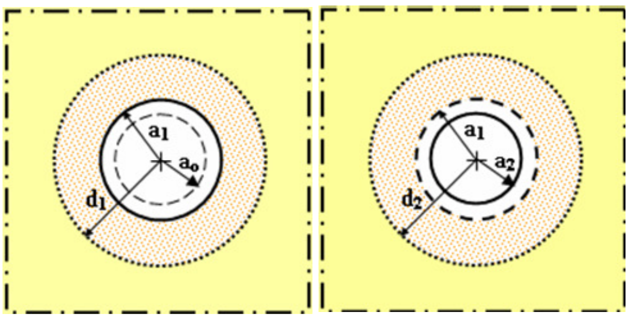

a) Expansion phase b) Contraction phase

Figure 1. Geometry of expansion and contraction phases.

The following are functions of the soil properties used in the derivation of the analytical solution in order to abbreviate the mathematical manipulation for both expansion and contraction phases.

$$\mathrm{G} = \frac{\mathrm{E}}{2(1+\upsilon)} \quad [1]$$

$$\alpha = \frac{(1+\sin\phi)}{(1-\sin\phi)} \quad [2]$$

$$\beta = \frac{(1+\sin\psi)}{(1-\sin\psi)} \quad [3]$$

$$\mathrm{Y} = \frac{2\,\mathrm{c}\cos\phi}{(1-\sin\phi)} \quad [4]$$

$$\delta = \frac{[\mathrm{Y}+(\alpha-1)\mathrm{P}_0]}{2(1+\alpha)G} \quad [5]$$

$$\gamma = \frac{\alpha(\beta+1)}{(\alpha-1)\beta} \quad [6]$$

$$\eta = \exp\left(\frac{(\beta+1)(1-2\upsilon)[\mathrm{Y}+(\alpha-1)\mathrm{P}_0](1+\upsilon)}{E(1-\alpha)\beta}\right) \quad [7]$$

$$\mu = \frac{1+\beta}{\alpha-1} \quad [8]$$

$$\iota = \frac{(\alpha-1)\,\mathrm{E}}{2(1-\upsilon^2)(\mathrm{Y}+(\alpha-1)\mathrm{P}_o)} \quad [9]$$

Where,
G is the shear modulus of the soil, α is a function of friction angle, β is a function of dilation angle, Y is a function of cohesion and friction angle, δ is a function of soil properties and the initial state of stress, P_o, while γ, η, μ, and ι are functions of the selected soil properties.

2.1 Expansion phase (loading case):

2.1.1 Elastic conditions

The radial cavity pressure, P (the additional pressure), at a given radius, a, during the elastic stage of expansion can be calculated by (Yu, et al 1991):

$$P = 2\mathrm{G}\delta + \mathrm{P}_\mathrm{O} \quad [10]$$

The radius, *a*, is then related to the initial cavity radius a_o by (Yu, et al 1991):

$$\frac{a}{a_o} = 1 + \frac{(\mathrm{P}-\mathrm{P}_o)}{2\mathrm{G}} \quad [11]$$

2.1.2 Elastic-plastic conditions

During the elastic-plastic stage, the radius of the interface between the elastic and plastic zones is given by:

$$\frac{d_1}{a} = R^{\frac{\alpha}{(\alpha-1)}} \quad [12]$$

Where d_1 is the radius of the plastic zone, R is the cavity pressure ratio given by Eq.14, and a is given by:

$$\frac{\mathrm{a}}{\mathrm{a}_\mathrm{o}} = \left[\frac{\mathrm{R}^{-\gamma}}{(1-\delta)^{\frac{(\beta+1)}{\beta}} - (\frac{\gamma}{\eta})\,A_1(R,\xi)}\right]^{\frac{\beta}{(\beta+1)}} \quad [13]$$

where

$$R = \frac{(1+\alpha)\,[\mathrm{Y}+(\alpha-1)\,\mathrm{P}]}{2\alpha[\mathrm{Y}+(\alpha-1)\,\mathrm{P}_0]} \quad [14]$$

and

$$\mathrm{A}_1(R,\ \zeta) = \sum_{\mathrm{n}=0}^{\infty}\mathrm{A}_n^1 \quad [15]$$

in which

$$A_n^1 = \begin{cases} \dfrac{y^n \ln x}{n!} & if \quad n=\gamma \\ \dfrac{y^n (x^{(n-\gamma)}-1)}{n!(n-\gamma)} & otherwise \end{cases} \quad [16]$$

where $A_1(R,\zeta)$ is an infinite series; A_n^1 is the general term of the series, x and y are variables representing (R,ζ) and n is the number of terms (Yu and Houlsby 1991).

2.2 Contraction phase (unloading case):

During the unloading stage, the cavity pressure decreases gradually from P to a value P-x (P-P_o), where 0 < x < (P-P_o). The soil unloads elastically until (Yu, et al 1995):

$$x_2 = \frac{[Y+(\alpha-1)P](1+\alpha)}{2\alpha(P-P_o)} \quad [17]$$

and

$$P_2 = \frac{[(1+\alpha)Y + \alpha(1+\alpha)P_o]}{(1+\alpha)} \quad [18]$$

where, x_2 is the factor at which the reverse yielding starts and P_2 is the cavity pressure that causes this yielding. All of the remaining factors have been discussed previously.

2.2.1 Elastic conditions

For any value of the unloading factor x up to the value x_2, the response of the soil is purely elastic and is given by (Yu and Houlsby 1995):

$$\frac{a_2}{a} = 1 - \frac{x(P-P_o)}{2G} \quad [19]$$

2.2.2 Elastic-plastic conditions

For an unloading factor x that exceeds the boundary factor x_2, yielding will be initiated and the response of the soil will follow elastic-plastic behaviour. The ratio of the radius of a given annulus to that of the plastic zone surrounding it is given by:

$$\frac{d}{d_2} = 1 + \frac{2(1+\alpha)\delta}{(1+\alpha)}\left(\frac{d_1}{d}\right)^{\frac{(\alpha-1)}{\alpha}} \quad [20]$$

where d is the position of the outer radius of the plastic zone during unloading and d_1 and d_2 are as defined previously.

The relationship between the radius of the cavity at any point in time, d, and the radius of the cavity at the end of the contraction phase, a_2, is a nonlinear equation in terms of a_2/d_2, i.e.,

$$\alpha A_2\left(\kappa, \frac{d}{a}\right) + \left(\frac{d_2}{d}\right)^{1+\beta} A_3\left(\lambda, \frac{a_2}{d_2}\right) = 0 \quad [21]$$

where,

$$\lambda = \frac{1}{(1+\alpha)\iota}\left[1 - \frac{\beta\upsilon}{1-\upsilon} + \alpha[\beta - \frac{\upsilon}{1-\upsilon}\right]\left(\frac{b}{d}\right)^{\frac{\alpha-1}{\alpha}} \quad [22]$$

$$\kappa = \frac{1}{(1+\alpha)\iota}\left[\alpha\left[1 - \frac{\beta\upsilon}{1-\upsilon}\right] + \beta - \frac{\upsilon}{1-\upsilon}\right]\left(\frac{b}{d}\right)^{\frac{\alpha-1}{\alpha}} \quad [23]$$

and $A_2(k, d/a)$ is an infinite series given by

$$A_2(x,y) = \sum_{n=0}^{\infty} A_n^2 \quad [24]$$

in which

$$A_n^2 = \begin{cases} \dfrac{x^n(\alpha-1)}{n!\,\alpha}\ln y & \text{if } n = \alpha\mu \\ \dfrac{x^n}{n!(n-\alpha\mu)}[y^{(\frac{\alpha-1}{\alpha})(n-\alpha\mu)} - 1] & \text{otherwise} \end{cases} \quad [25]$$

Finally, $A_3(\lambda, a_2/d_2)$ is a nonlinear infinite series given by (Yu and Houlsby 1995):

$$A_3(x,y) = \sum_{n=0}^{\infty} \frac{x^n}{n!(n+\mu)}(y^{(\alpha-1)(n+\mu)} - 1] \quad [26]$$

3 NUMERICAL MODEL

The main objectives of this section are two folds: first to verify the capabilities of the finite element model to capture the response of the tackled problem, which involves high level of expansion reaching up to 50% (i.e., a/ao=1.5), and to investigate the effect of deviation from the assumptions of the analytical solution on its predictions. The first objective is achieved by examining a finite element model (Mesh 1) that has the same geometric and loading conditions as that of the analytical solution (i.e. infinite medium and constant isotropic stress field everywhere). The second objective will be accomplished in two steps: a) use Mesh 1 to study the effect of stress anisotropy (i.e. Ko≠ 1) and to validate the finite element model (Mesh 2); b) use Mesh 2 to perform a parametric study to investigate the effect of embedment depth (i.e. free surface condition) on the accuracy of the analytical solution. For the latter case, a mesh with a very high burial depth, cover to diameter ratio, C/D = 40 (Mesh 2) was used to minimize the free surface effects during the validation process.

3.1 Finite Element Mesh and Its Verification

The fifteen-nodded cubic strain triangular elements finite element included in the element library of the FE package PLAXIS was used to simulate the expansion and contraction phases of a plane strain cylindrical cavity subjected to radial internal pressure. Taking advantage of symmetry for both meshes, only the right half of the problem was modeled. The lateral and bottom boundaries were placed about 40 times the diameters to simulate the infinite medium. The size of the model was selected such that the artificial boundaries and boundary conditions would not affect the ground stresses around the cavity. The problem geometry and the FE Mesh 1 are shown in Figure 2; whereas, Figure 3 shows Mesh 2.

The Mohr-Coulomb failure criterion (i.e. elasto-plastic stress-strain relationship) was used as the constitutive model for the ground. The criterion assumes a linear elastic soil behavior up to the defined Mohr-Coulomb failure surface. If the failure surface is reached, the soil yields, with corresponding stress redistribution to maintain equilibrium, up to the point where the stress conditions in the soil zones do not violate the yield surface and become, again, acceptable under the failure criterion. The material was modeled as purely frictional soil (i.e. c = 0) with the following properties: Young's modulus, E = 20 MPa, Poisson's ratio, v = 0.25, angle of friction, ϕ= 30º and angle of dilatation, ψ = 13º.

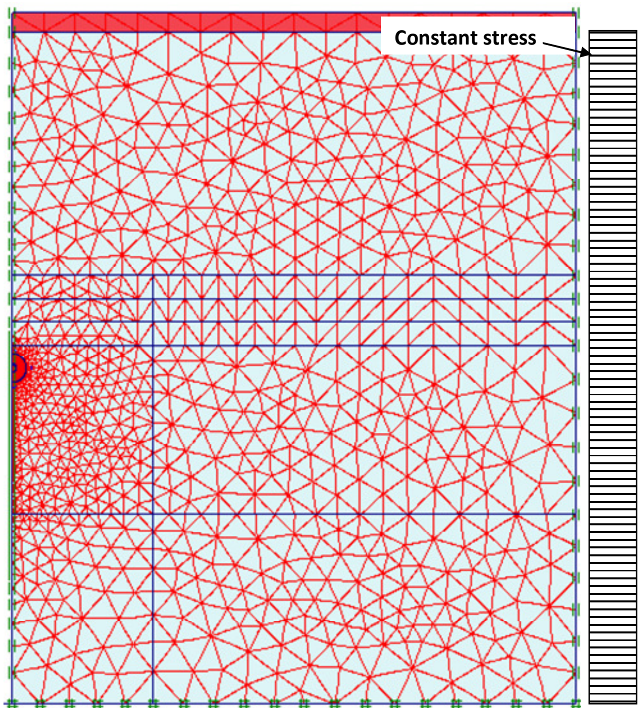

Figure 2. Problem geometry and the FE Mesh 1

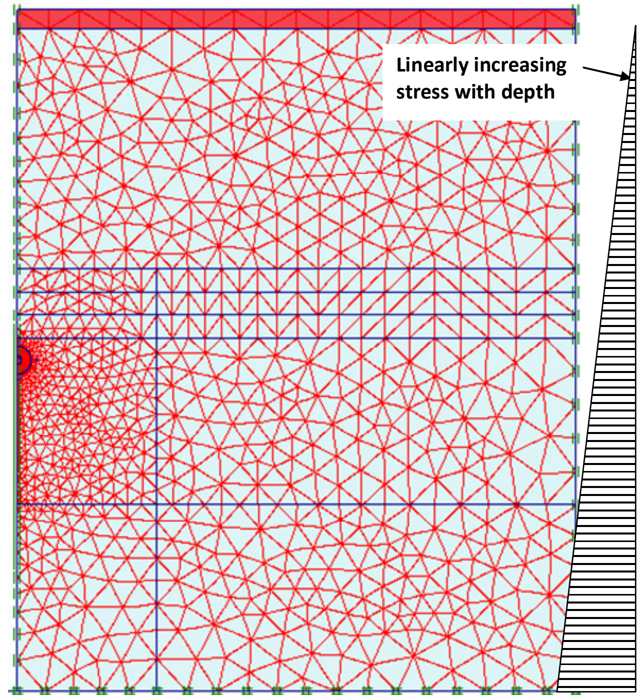

Figure 3. Problem geometry and the FE Mesh 2

3.1.1 Validation Results

Mesh 1

As mentioned above, this mesh has the same geometric and loading conditions as that of the analytical solution. The cavity was assumed to expand to a/ao=1.5. Upon reaching this level of expansion, the cavity was assumed to contract back. Figure 4 compares the relationship between radial cavity pressures normalized by initial soil pressure P/P_o versus cavity radius normalized by the initial cavity radius a/a_o calculated from the FE to that obtained from the analytical solution. As it can be noted from Figure 4, there he FE predictions agree well with the results of the closed form solution. This demonstrates the ability of the numerical model to capture the response of the tackled problem and the suitability of the mesh size. Therefore, it can be used to study the effect of stress anisotropy on the predictions of the analytical solution.

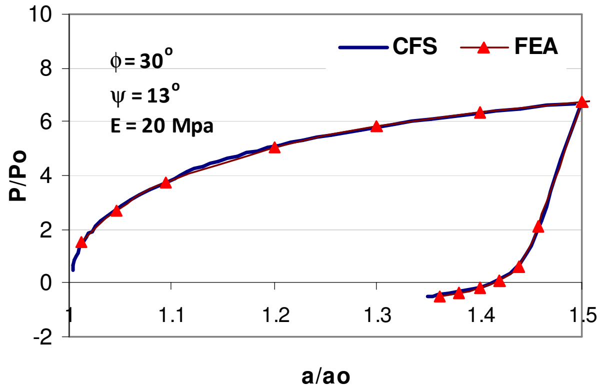

Figure 4. Radial cavity pressure normalized by initial soil pressure, P/P_o, versus the cavity radius normalized by the initial cavity radius, a/a_o, for loose sand.

Mesh 2

This mesh will be used in the subsequent section to study the effect of the embedment depth. To verify this mesh, a cavity embedded at cover to diameter ratio, C/D = 40 was tested. The cavity was expanded to a/ao=1.5. The internal pressures were then relieved to simulate the contraction phase. Figure 5 compares the relationship between radial cavity pressures normalized by initial soil pressure P/P0 versus cavity radius normalized by the initial cavity radius a/a0 calculated from the FE to that obtained from the analytical solution. The results of the closed form solution are within 2% from that obtained from the FE predictions. This implies that at high burial depths, the effect of the assumption of infinite depth (i.e. neglecting the effect of free surface) on the closed form solution (CFS) results is negligible.

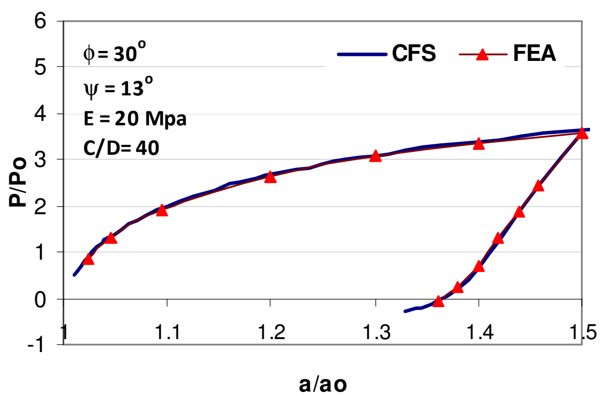

Figure 5. Radial cavity pressure normalized by initial soil pressure, P/P_o, versus the cavity radius normalized by the initial cavity radius, a/a_o, for C/D=40.

4 EFFECT OF THE FREE SURFACE AND THE STRESS GRADIENT

This section presents the results of an extensive parametric study conducted to explore the effect of the free surface situation (embedment depth) on the predicted response from the closed form solution by comparing its results to that obtained from the finite element calculations.

In the parametric study, the cavity expansion was assumed to reach 150% (i.e., the expanded diameter is 1.5 times the original diameter). The contraction stage was assumed to start after an expansion ratio, a/a_o = 1.1, 1.3, and 1.5 was reached. In other words, the upsizing ratios were assumed to be 10, 30 and 50%, respectively.

Figures 6, 7 and 8 display the radial cavity pressures normalized by the initial soil pressure, P/P_o, versus the cavity radius normalized by the initial cavity radius, a/a_o, for loose sand for buried depths that vary from C/D = 20 to C/D = 5. It can be noted from Figures 6 to 8 that the relationship between cavity pressure and its radius during the expansion phase is nonlinear. The initial part of the contraction phase remains linear until 85% of the expansion pressure has been relieved, followed by a strongly nonlinear zone. For C/D = 20, the predictions of the analytical solution are close enough to that obtained from the FE calculations as shown in Figure 6 (within less than 3% difference). Thus, it can be noted that up to embedment depth of C/D = 20, the closed form solution can predict the behaviour with reasonable accuracy. However, as the embedment depth decreases, the free surface effects are clearly manifested as can be seen from Figure 7, which presents the results for the case of C/D = 10. In this case the difference between the closed form solution and the FE results is 16% for expansion ratio, a/a_o = 1.3, and reaches up to 24% for a/a_o = 1.5. For embedment depth of C/D = 5, the trend of disagreement is even worse as it can be noted from Figure 8, the magnitude of difference escalates to 34% for expansion ratio, a/a_o = 1.3, and reaches up to 37% for a/a_o = 1.5.

As it can be noted from the results of the parametric study, during the expansion phase the closed form solution overestimates the required cavity pressure to expand the cavity. This is due to the increased resistance implied by the assumption of the closed form solution that the stress field is constant to an infinite distance in every direction. Whereas, in the simulated real case (i.e. the FE model) the stress decreases towards the surface till it vanishes at the free surface. Thus, the resistance to cavity expansion is less and, therefore, the needed pressure to expand the cavity is less. This is more prevalent for C/D ratios ≤ 10 or less.

Based on the results of the contraction phase, it can be deduced that as the closed form solution overestimates the cavity pressure in the expansion phase, the cavity pressure at the start of the unloading phase is also overestimated. As a result, the slope of the unloading curve increases, leading to further underestimation of the cavity pressure during unloading.

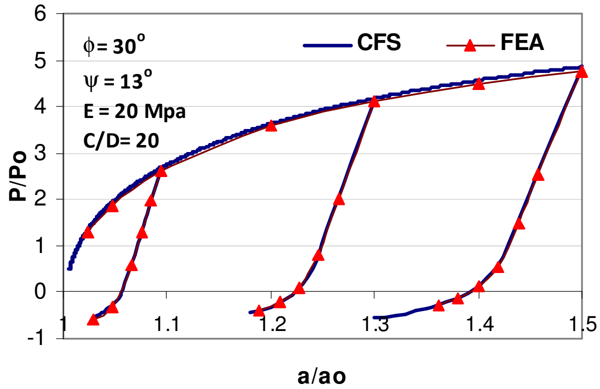

Figure 6. Radial cavity pressure normalized by initial soil pressure, P/P_o, versus the cavity radius normalized by the initial cavity radius, a/a_o, for C/D=20.

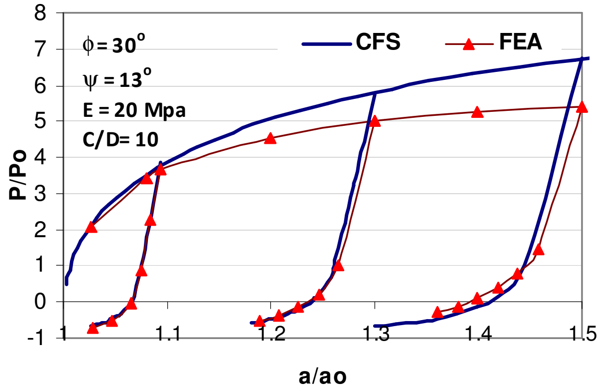

Figure 7. Radial cavity pressure normalized by initial soil pressure, P/P_o, versus the cavity radius normalized by the initial cavity radius, a/a_o, for C/D=10.

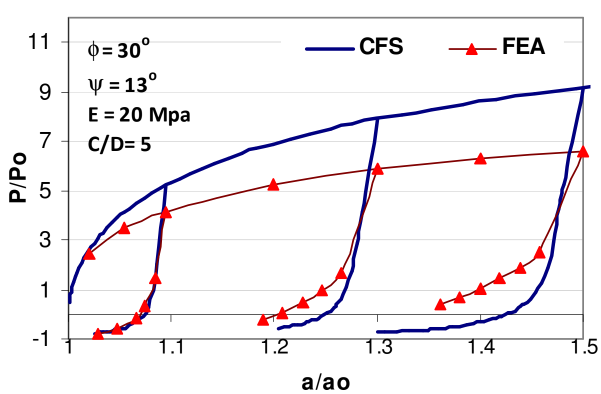

Figure 8. Radial cavity pressure normalized by initial soil pressure, P/P_o, versus the cavity radius normalized by the initial cavity radius, a/a_o, for C/D=5.

5 EFFECT OF THE IN-SITU STRESS ANISOTROPY

This section presents the results of the study conducted to investigate the effect of the in-situ stress anisotropy (i.e. Ko≠ 1) on the displacements during expansion and contraction phases of cavities embedded in dilatant sands. The calculated results of FE analysis are compared to the predicted response of the closed form solution to study the magnitude of approximation that may introduced by the closed form solution for such cases (i.e. Ko≠ 1).

In order to separate the effect of in-situ stress anisotropy from the influnce of the embedment depth and the stress gradient Mesh 1 was utilized. As mentioned earlier, Mesh 1 has the same geometric and loading condition as that of the analytical solution.

In the study, three different values for the coefficient of lateral earth pressure at rest, K_o, were considered (K_o=1.0, 0.8, and 0.5). The cavity expansion was assumed to reach 150% (i.e., the expanded diameter is 1.5 times the original diameter). The contraction stage was assumed to start after an expansion ratio, a/a_o = 1.1, 1.3, and 1.5 was reached. Thus, the upsizing ratios were assumed to be 10, 30 and 50%, respectively.

For the in-situ isotropic stress state case (K_o= 1.0), there is a perfect agreement between the FE predictions and the closed form solution results at all expansion and contraction level as shown in Figure 9. This agreement starts to deteriorate for cases involved the in-situ stress anisotropy as shown in Figures 10 and 11. As it can be seen from Figure 10 for the case of K_o= 0.8, the closed form solution overestimates the cavity pressures during the expansion phase by up to 10% and during the contraction phase by 14%. Even worse, for the case of K_o= 0.5 the closed form solution over predicts the cavity pressures during expansion by up to 40% and during the contraction by 55%. This trend is expected and is related to the early onset of yielding as the confining stress decrease for cases were Ko≠1.0 . thus, a smaller amount of cavity pressure results in a larger cavity displacements.

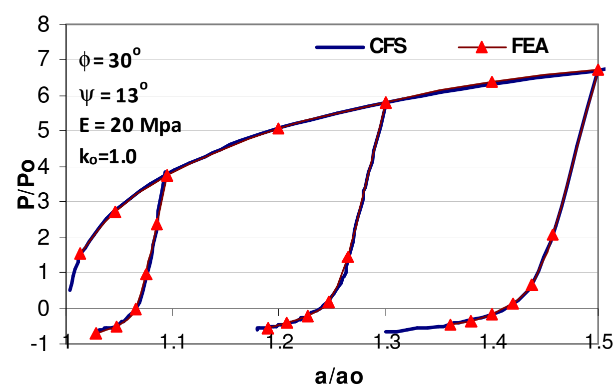

Figure 9. Radial cavity pressure normalized by initial soil pressure, P/P_o, versus the cavity radius normalized by the initial cavity radius, a/a_o, for K_o =1.0.

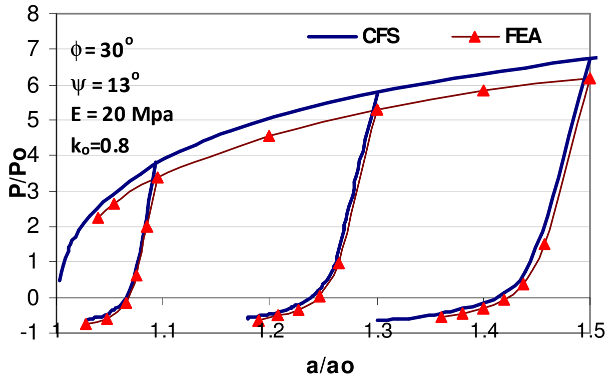

Figure 10. Radial cavity pressure normalized by initial soil pressure, P/P_o, versus the cavity radius normalized by the initial cavity radius, a/a_o, for K_o =0.8.

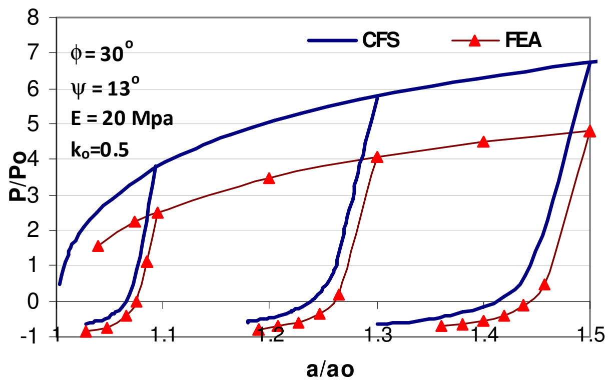

Figure 11. Radial cavity pressure normalized by initial soil pressure, P/P_o, versus the cavity radius normalized by the initial cavity radius, a/a_o, for K_o =0.5.

6 CONCLUSIONS

The results obtained in this study show that the closed form solution for cavity expansion can be used reliably to evaluate the cavity pressures for up to an embedment depth, C/D = 20. However, as the embedment depth decreases, the free surface affects its accuracy substantially. For the case of C/D = 10, the difference between the closed form solution is as high as 24% for a/a_o = 1.5 and the difference reaches 37% for C/D = 5. The results also showed that the stress anisotropy conditions can have significant effects on the results of the closed form solution. For example, for K_o= 0.8, the closed form solution overestimates the cavity pressures during the expansion phase by up to 10% and during the contraction phase by 14%. For the case of K_o= 0.5, the closed form solution overpredicts the cavity pressures during expansion by up to 40% and during the contraction by 55%. These differences can have significant implications when evaluating the forces associated with HDD installations and the selection of the necessary equipment, which may impact the economic feasibility of the HDD installation. It is therefore necessary to correct the predicted pressure values to account for effects of embedment and stress anisotropy.

REFERENCES

El Naggar, M.H. and Sakr, M. 2000. Evaluation of axial performance of tapered piles from centrifuge tests. Canadian Geotechnical Journal, 37(6): 1295-1308.

Fernando, V. and Moore, I.D. 2002. Use of cavity expansion theory to predict ground displacement during pipe bursting. Proc. of Pipelines 2002, ASCE, Cleveland, OH, July, 11pp

Gibson, R. E. & Anderson, W. F. 1961. In situ measurement of soil properties with the pressuremeter. Civil Engineering Public Works Rev. 56: 615-618.

Hughes, J. M. O., Wrath, C. P. & Windle, D.1977. Pressuremeter tests in sands. *Geotechnique*, 27(4): 455-477.

Palmer, A. C. (1972). Undrained plane-strain expansion of a cylindrical cavity in clay: a simple interpretation of the pressuremeter test. *Geotechnique* 22(3): 451-457.

Randolph, M. F., Carter, J. P. & Wrath, C. P.1979. Driven piles in clay--the effects of installation and subsequent consolidation. *Geotechnique* 29(4): 361-393.

Yu, H.S and Houlsby, G.T. 1991. Finite cavity expansion in dilatant soils: loading analysis. *Geotechnique*, Vol. 41:173-183.

Yu, H.S. and Houlsby, G.T. 1995. A large strain analytical solution for cavity contraction in dilatant soils. International Journal for Numerical and Analytical Methods in Geomechanics, Vol. 19:793-811.

Yu H.S. and Rowe R.K.1999, Plasticity solutions for soil behaviour around contracting cavities and tunnels. International Journal for Numerical and Analytical Methods in Geomechanics, Vol. 23: 1245-1279.

Yu H.S. and Carter, J.P. 2002. Rigorous similarity solutions for cavity expansion in cohesive-frictional soils. International Journal of Geomechanics, Vol. 2(3).